ERURJ **2023**, 2, 3, 374-384

(Article)

Substrate Integrated Waveguide Based Magneto-Electric Antenna for 5G

Mohamed A. Asal[1*], *Saber H. Zainud-Deen*[2], *Hend Malhat*[2], *and Shaymaa.M.gaber*[1]

[1]*Telecommunication Engineering Department, Faculty of Engineering, Egyptian Russian University, Badr City, Cairo, Egypt.*

[2]*Faculty of Electronic Engineering, Menoufia University, Egypt.*

*Corresponding author(s): Mohamed Asal, E-mail: mohamed-asal@eru.edu.eg, Tel: +201067446855

Received 22nd February 2023, Revised 29h April 2023, Accepted 8th May 2023.

DOI:10.21608/ERURJ.2023.193322.1013

ABSTRACT

This paper introduces a wideband magneto-electric (ME) antenna with radiation characteristics for 5G communications. The antenna consists of two horizontal patches as an electric dipole printed on a silicon oxide substrate arranged horizontally and five vertical pins as a magnetic dipole. The substrate is deposited on a copper ground with two cavities at the corners, each of which includes 13 pins. The substrate-integrated waveguide (SIW) ME-antenna is fed with a 50 Ω SMA connector placed below a cavity ground plane with two openings at the corners. The single element has an impedance-matching bandwidth of 25% with a circularly polarised band of 8%. The effect of the cavity is studied. The mutual coupling between ME-antenna elements is investigated for linear and circular arrangements. In order to improve the maximum gain and the circular polarisation (cp) bandwidth of the proposed SIW ME-dipole antenna, a sequentially fed 2x2 ME-dipole antenna array is investigated. The 4-element array introduces a high gain of 11.95 dBi. The 16 elements of the SIW ME dipole antenna array enhance the gain from 8.3 dBi to 17.73 dBi. The proposed antenna structures are implemented and analysed using the finite integral technique (FIT).

Keywords: Substrate integrated waveguide, Circular polarization, Magneto-Electric antenna.

1. Introduction

Substrate-integrated waveguide (SIW) technology has emerged as a viable alternative to traditional all-metal waveguides during the last decade. It is utilised in the design of components for microwave and millimetre-wave communication systems [1]. Its unique construction is composed mostly of two parallel metal plates, a dielectric substrate, and a sequence of metallic vias. By changing the distance between metallic vias, the effect of bandgap loss may be minimised. On the one hand, the SIW construction preserves the benefits of classic waveguides, such as high quality factor and high power capacity, while significantly lowering circuit size. Additionally, because it is easy to interact with other devices, no transitions between components are required, making the entire system less lossy. As a result, SIW technology offers benefits in small size, cheap cost, low loss systems, and minimises the entire transition need. In recent wireless communications, 5G Wi-Fi has grown in popularity. Its operational frequency ranges from 24 to 40 GHz. Due to their excellent electrical characteristics, such as wide bandwidth, low back radiation, and symmetrical radiation patterns across the entire operating frequency range, magneto-electric (ME) dipole antennas can be used in a variety of wireless communications, including base station antennas for mobile communications [1], ultra-wideband systems [5], and millimetre-wave radio [6]. The downside of these typical ME-dipoles is their high profile of 0.25 λ. Folded structures [7], [9], or loaded with dielectric materials [10] were proposed to minimise height. Despite the fact that these antennas [7] and [10] have low-profile and wideband characteristics, they are challenging to realise at high frequencies. When the operating frequency is increased, the antenna size decreases. It is difficult to appropriately combine the -shaped feeding probes and the dielectric substrate block within a compact size, especially for the antenna design in [10]. The design of a ME dipole antenna in [1] is a combination of a half-wavelength electric dipole and a quarter-wavelength patch antenna. The height of the ME dipole antenna is equal to the length of the quarter-wavelength patch. Therefore, shortening the physical length of the quarter-wavelength patch means reducing the height of the ME dipole antenna. Folding the parallel walls into different shapes along the z-axis [7–9] can achieve this goal. An example of the folding technique is shown in Fig. 1(b). However, this approach is hard to fabricate. Folding a metal plate into multiple sections is challenging. In this communication, it is found that the current direction can be folded along the x-axis, and the fabrication process can be simplified. It can be done by cutting a pair of slots on the ground plane. The equivalent circuit of the proposed antenna is shown in Fig. 1(c). The proposed antenna structures are analysed using the finite integral technique (FIT) [4]. Table I. Some of them are circularly polarised, and some of them are linearly polarised.

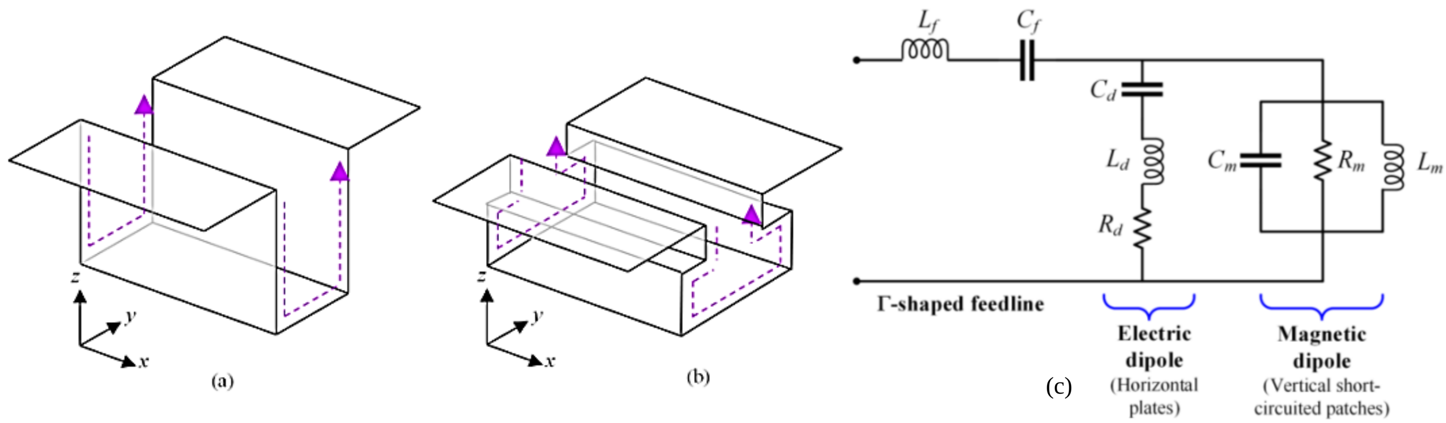

Fig.1. Vertical current direction of (a) conventional ME dipole antenna (b) ME dipole antenna with folded parallel walls structure in ref [7] and ref [8] (c) equivalent circuit.

2. Experimental

Design of SIW ME-antenna

A wideband SIW ME antenna with reconfigurable radiation characteristics is designed and optimised for 5G communications. The geometry of the proposed antenna is shown in Fig. 2. It consists of two horizontal patches as an electric dipole printed on a silicon oxide substrate with r = 3.9 and thickness t = 1.34 mm and five vertical pins as a magnetic dipole. The substrate is deposited on a copper ground with two cavities at the corners, each of which includes 13 pins. The SIW ME-antenna is fed with a 50 Ω SMA connector placed below a cavity ground plane with two openings at the corners. The optimised dimensions of the SIW antenna are (in millimetres): L = 15.2, S = 5, rpin = 0.2, spin = 0.15, spincavity = 0.7, a = 2.1, R1 = 2.46, R2 = 1.135, and b = 0.82. This antenna is designed and optimised for 5G applications in the frequency band from 25 GHz up to 40 GHz.

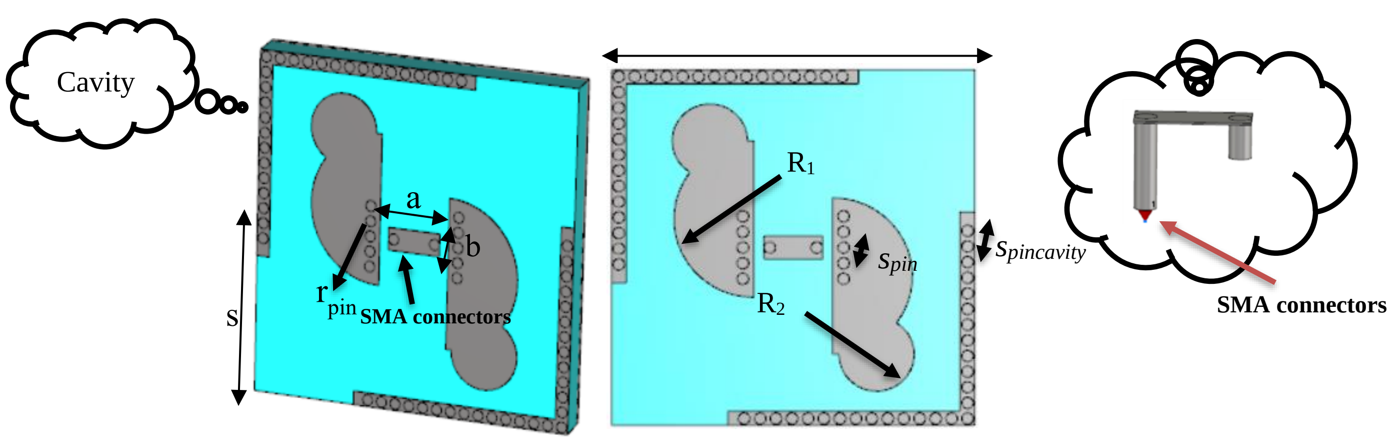

Figure 2. The structure of the SIW ME antenna element at L=15.2, S=5, r_{pin}=0.2, s_{pin}=0.15, $s_{pincavity}$=0.7, a=2.1, R_1=2.46 ,R_2=1.135 and b=0.82.

Ref.	**Antenna Figure**	**Size (mm)**	**Bandwidth** (S11< -10dB)	**Gain** (dBi)	**CP-BW** (AR<3dB)	**Polarization**
[11]	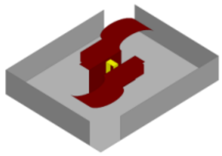	145x180x30	1.76 to 3.46 GHz (65%)	8±1	1.68 to 3.55 GHz (71.5%)	Circular
[12]	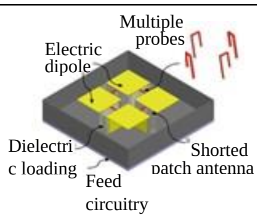	150x150x18	1.65 to 2.12 GHz	8.2	48 %	linear
[12]	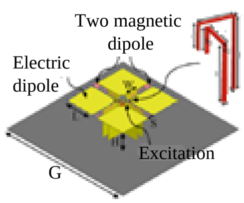	149.6x149.6 x28	1.7185 to 3.409 GHz	9	45%	linear
[13]	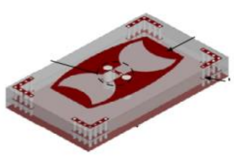	32.5x62x8	3.1-10.66 GHz **(**110%**)**	8.4± 2.5	3.1-10.66 GHz	linear
[14]	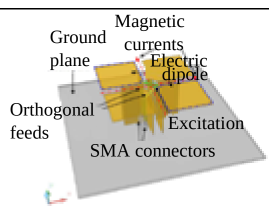	110x110x36	1.69 to 2.76 GHz	7.6 to 9.4	1.23 to 3.23 GHz (90%)	circular

Table I: ME dipole antenna examples.

The frequency response of the ME-antenna is investigated and plotted in Fig. 3. It maintains an impedance-matched BW frequency range from 28 to 36 GHz, as illustrated in Fig. 3a. The antenna introduces a high gain of 8 dBi, as shown in Fig. 3b and Fig. 3c. The CP radiation with AR3 dB is achieved from 27.4 GHz to 29.9 GHz.

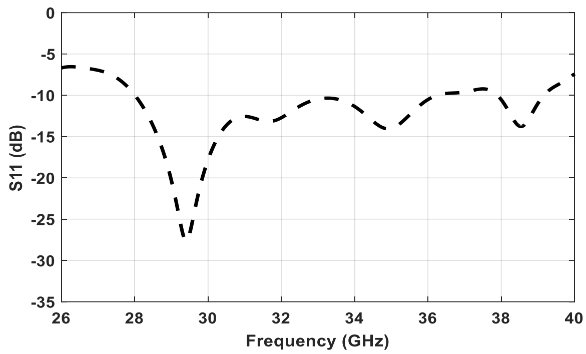

a. Reflection coefficient

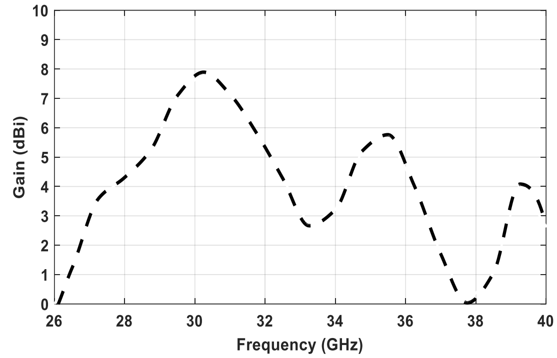

b. Gain

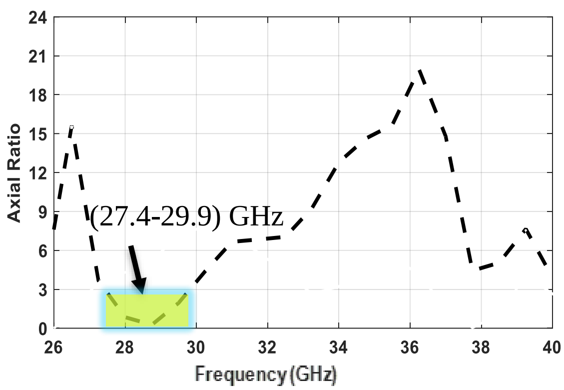

c. Axial-ratio

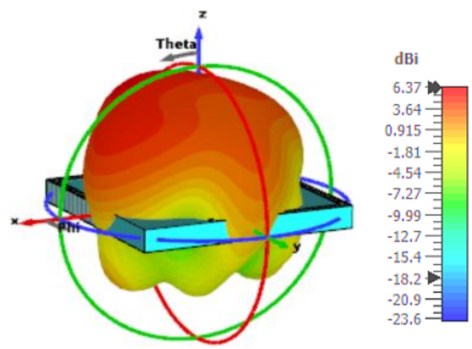

d. 3D gain at 29 GHz

Figure 3. The radiation characteristics of the SIW ME-antenna element.

3. Results and discussion

Effect of the cavity geometry

The effect of the cavity is studied; ME antennas are taken without a cavity and with a cavity with two openings, as shown in Figs. 4 (a,b). Figure 5 shows that the ME without cavity has no resonant frequency in the band from 26 to 40 GHz, but the cavity-covered BW has a frequency range from 28 to 36 GHz. and the peak gain is raised from 6 dB to 8 dB by adding a cavity of two openings to the ground plane at f = 28 GHz.

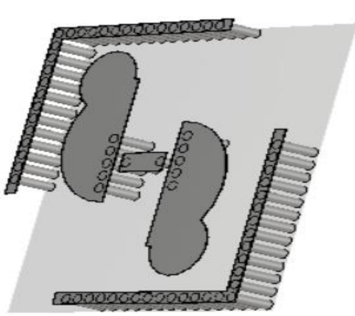

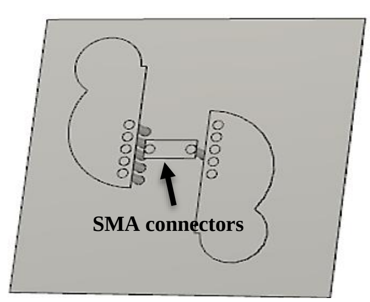

a.with cavity of two opening b.without cavity

Figure 4. The geometry of cavity shape.

The two openings in the cavity increase the CP bandwidth to cover the frequency range from 27.4 GHz to 29.9 GHz. This occurs due to the reduction in back radiation and the cavity walls. But without a cavity, there is no CP bandwidth.

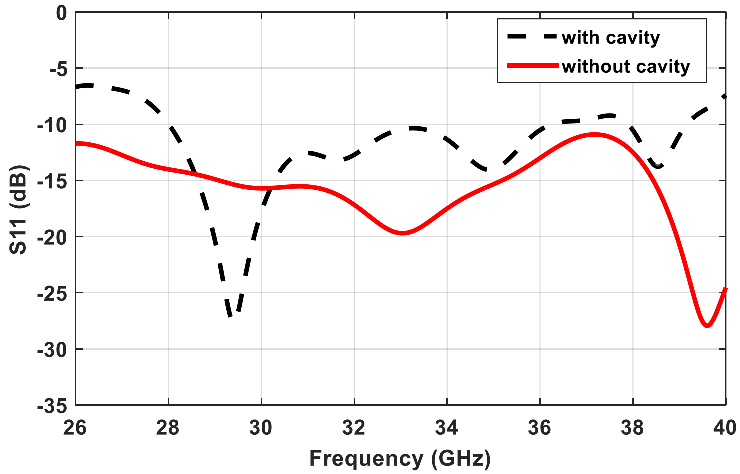

a. Reflection coefficient

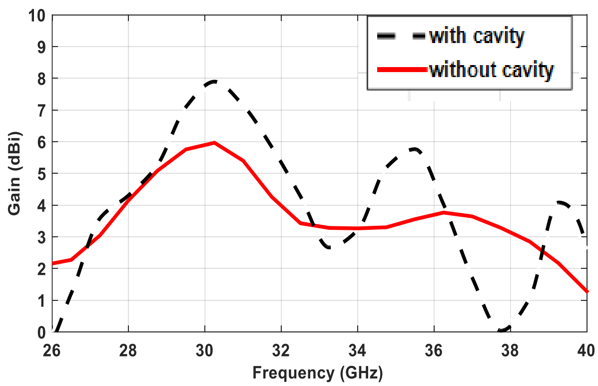

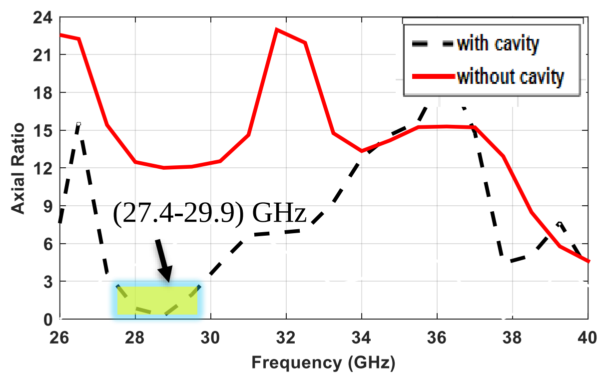

b. Gain

c. Axial-ratio

Figure 5. The effect of cavity shape at L=15.2, S=5, r_{pin}=0.2, s_{pin}=0.15, a=2.1, R_1=2.46 ,R_2=1.135 and b=0.82.

ME-Dipole Antenna Array

To maximize the peak gain and CP bandwidth of a single antenna element, array designs with sequential feeding are employed. Figure 6 depicts a unit-pair consisting of two ME-dipole antennas separated by a distance L and fed with identical magnitudes, a 90° phase shift, and rotated 90° relative to each other. It maintains an impedance-matching wide BW of 27.6% across the unit-pair frequency range from 27.8

to 36.7 GHz, as illustrated in Fig. 7a. Figure 7b shows the peak gain increased from 8 to 8.9 dBi at f =30.3 GHz. As demonstrated in Fig. 7c, CP radiation with an AR > 3 dB is produced from 27.1 GHz to 30.9 GHz.

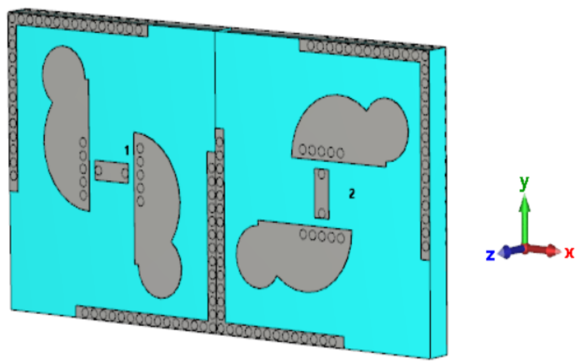

Figure 6. The arrangement 2x1 of ME-dipole antenna array at L=15.2, S=5, r_{pin}=0.2, s_{pin}=0.15, $s_{pincavity}$=0.7, a=2.1, R_1=2.46, R_2=1.135 and b=0.82.

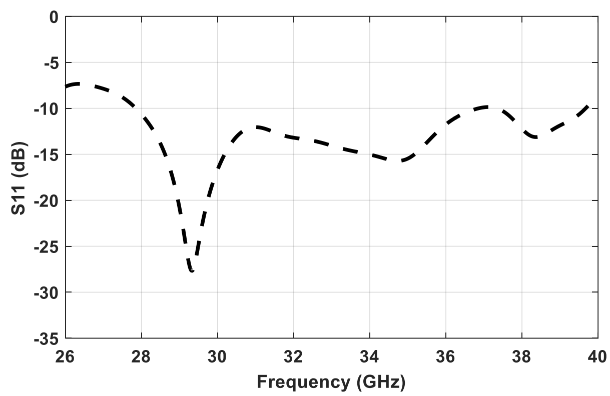

a. Reflection coefficient

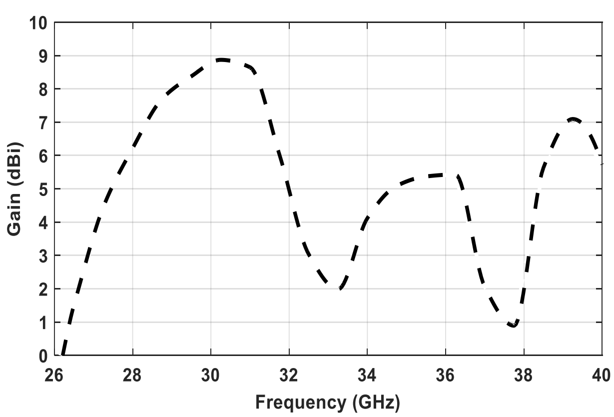

b. Gain

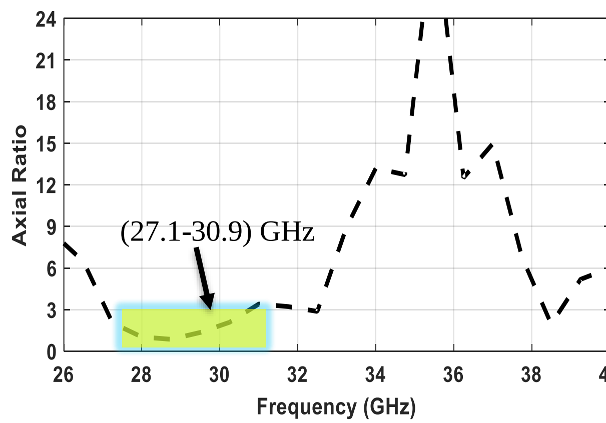

c. Axial-ratio

Figure 7. The radiation characteristics of the unit-pair arrangement.

A sub-array consisting of 2 × 2 sequentially fed antenna elements is investigated in Fig. 8. The sub-array elements are rotated by 90° to achieve an orthogonal field component with equal amplitude. The peak gain increases from 8 dBi for a single element to 12 dBi. Figure 9 a, b, and c show the reflection coefficient covering the frequency range from 27.8 to 37 GHz, gain, and AR of the SIW ME antenna element. The CP radiation with AR3 dB is achieved from 27 GHz to 33 GHz, as shown in Fig. 9c. The gain has improved to 12 dBi. The 2 × 2 ME-dipole sub-array is used as a building block for different array configurations. The beam-switching arrays are designed to produce single or multiple beams in different directions.

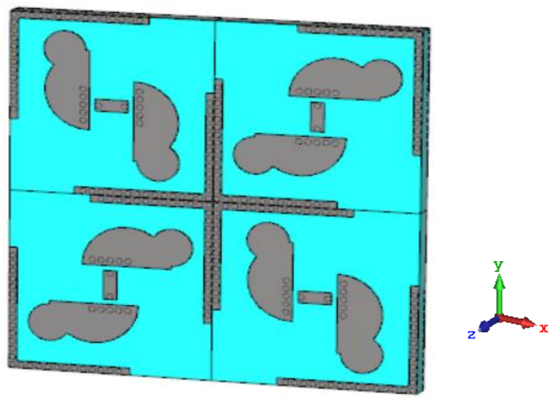

Figure 8. The arrangement 2x2 of ME-dipole antenna array at L=15.2, S=5, r_{pin}=0.2, s_{pin}=0.15, $s_{pincavity}$=0.7, a=2.1, R_1=2.46 ,R_2=1.135 and b=0.82.

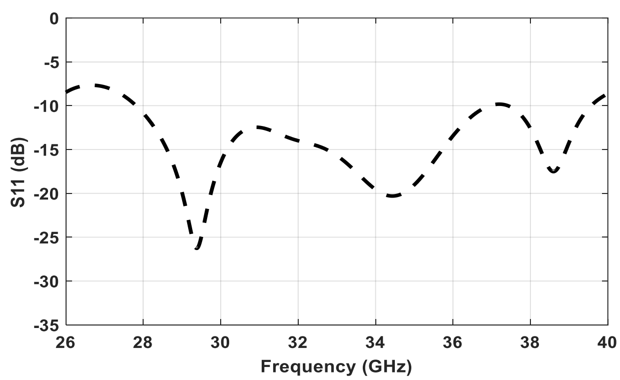

a. reflection coefficient

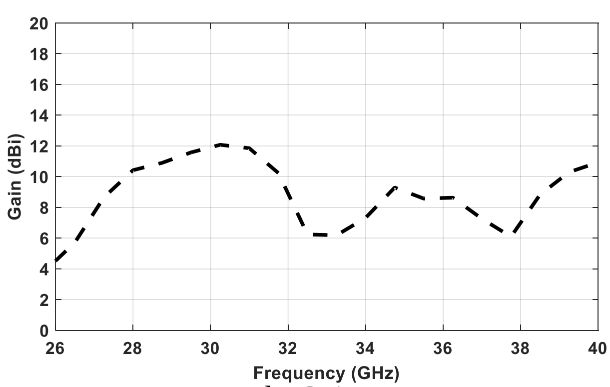

b. Gain

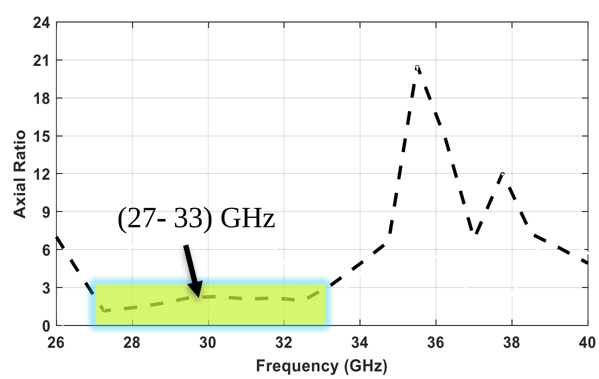

c. Axial-ratio

Figure 9. The radiation characteristics of the 2 × 2 array.

An arrangement comprising 16 ME-dipole elements, compromising four 2 × 2 sub-arrays, is investigated for gain improvement as shown in Fig. 10. The far-field frequency response of the SIW ME antenna element is shown in Figs. 11 a, b, and c. A directive pattern with 17.9 dBi is achieved with a high front-to-back ratio and low side lobe level. the 2 × 2 sub-array to each element, covering the frequency range from 28 to 40 GHz. The peak gain increases from 8 dBi for a single element to 12 dBi for the 2 × 2 sub-array and to 17.9 dBi for a 4 × 4 4 array. The CP radiation is maintained over the frequency band from 27.8 GHz to 34.1 GHz.

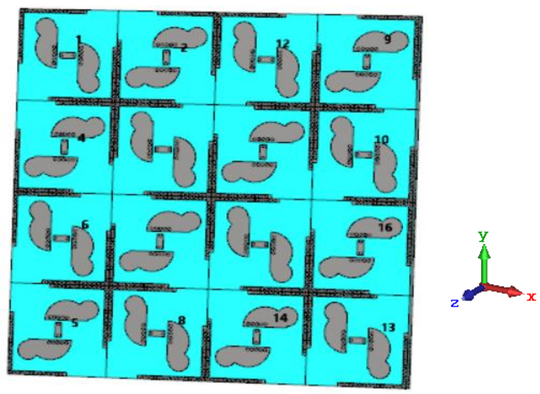

Figure 10. The arrangement 4x4 of ME-dipole antenna array at L=15.2, S=5, r_{pin}=0.2, s_{pin}=0.15, $s_{pincavity}$=0.7, a=2.1, R_1=2.46 ,R_2=1.135 and b=0.82.

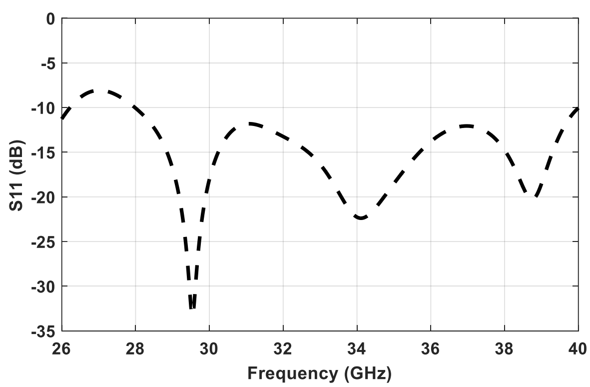

a. Reflection coefficient

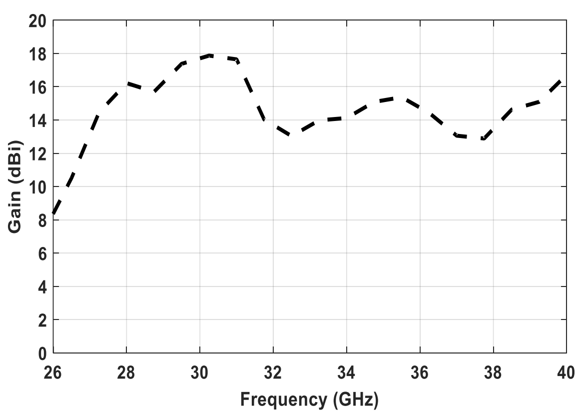

b. Gain

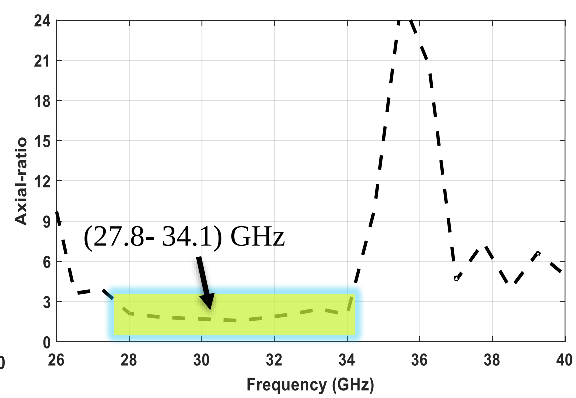

c. Axial-ratio

Figure 11. The radiation characteristics of the 4× 4 array.

The single ME-dipole has a matching bandwidth of 28–36 GHz. A 2 × 2 ME-dipole subarray is designed to increase the CP bandwidth to 21% with a peak gain of 17.73 dBi. In order to improve the maximum gain and the CP bandwidth of the proposed SIW ME-dipole antenna, a sequentially fed 2x2 ME-dipole antenna array is investigated. Different array arrangement characteristics have been investigated in Table II.

Table II: Different array arrangements of proposed ME dipole antenna.

	1 Element	2 Element	2*2 element	4*4 element
S11 (Band width)	28 to 36 GHz	27.8 to 36.7 GHz	27.8 to 37 GHz	28 to 40 GHz
Gain (dBi)	8 dBi	8.9 dBi	11.95 dBi	17.73 dBi
Axial Ratio (dB)	27.4 to 29.9 GHz **[8.8 %]**	27.1 to 30.9 GHz **[13 %]**	27 to 33 GHz **[20 %]**	27 to 33 GHz **[21 %]**

4. Conclusion

The radiation characteristics of wideband ME antennas are investigated. The antenna introduces wideband impedance matching from 26 GHz to 40 GHz. A SIW high-gain CP ME-dipole antenna is designed. The simulated results show that the designed antenna has a maximum realised gain of about 8.3 dBi. The SIW antenna provides directional patterns, relatively flat gain, and a high radiation efficiency of 80% through the frequency band of interest, which makes it a good candidate for future 5G communication systems. The 4-element array introduces a high gain of 11.95 dBi. The 16-element SIW ME dipole antenna array enhances the gain from 8.3 dBi to 17.73 dBi.

5. References

[1] K. M. Luk and H. Wong, "A New Wideband Unidirectional Antenna Element," Int. J. Microw. Opt. Technol., vol. 1, no. 1, pp. 35–44, 2006.

[2] W. X. An, H. Wong, K. L. Lau, S. F. Li and Q. Xue, "Design of Broadband Dual-Band Dipole for Base Station Antenna," IEEE Trans. Antennas Propag., vol. 60, no. 3, pp. 1592–1595, Mar. 2012

[3] S. Fakhte, M. Zahir Joozdani, and D. Zarifi, Magneto-electric Dipole Antenna for 5G. In: Matekovits, L., Kanaujia, B.K., Kishor, J., Gupta, S.K. (eds) Printed Antennas for 5G Networks. PoliTO Springer Series. Springer, Cham, 2022.

[4] L. Zhao, Y. Li, J. Wang and L. Ge, "A Study on Millimeter-Wave Magneto-Electric Dipole Phased Arrays for 5G Dual-Band Applications," in IEEE Transactions on Antennas and Propagation, vol. 71, no. 3, pp. 2375-2384, March 2023.

[5] Y. Sun and J. Xu, "Millimeter-Wave Ultrawideband and Gain Enhancement Planar End-fire Antenna," 2022 International Applied Computational Electromagnetics Society Symposium (ACES-China), Xuzhou, China, pp. 1-3 , 2022.

[6] K. B. Ng, H. Wong, K.K. So, C. H. Chan, and K. M. Luk, “60 GHz Plated Through Hole Printed Magneto-Electric Dipole Antenna,” IEEE Trans. Antennas Propag., vol. 60, no. 7, pp. 3129–3136, Jul. 2012.

[7] M. -S. Liang, Y. Zhou, X. -S. Yang and P. -F. Wu, "A Low-Profile Dual-Polarized Substrate Integrated Magneto-Electric Dipole MIMO Antenna," in IEEE Antennas and Wireless Propagation Letters, 2023.

[8] Y. Zhu, Q. Tan, and K. Fan, “A Low-Profile Dual-Polarized Magneto-Electric Dipole Antenna for 5G Applications”. Appl. Sci. 2023.

[9] K. M. Luk and B. Wu, “The Magnetoelectric Dipole A Wideband Antenna for Base Stations in Mobile Communications ,” Proceedings of the IEEE, vol. 100, no. 7, pp. 2297-2307, 2012.

[10] Y.; Wang, W.; Tan, K.; Zhu, H.; Luo, G.; Zhao, and H. Sun, “Design of A Ka-band 3D-printed dual-polarization magnetoelectric dipole antenna array with low sidelobe”. *Electronics* **2021**.

[11] J. Wang et al., "A low-profile vertically polarized magneto-electric monopole antenna with a 60% bandwidth for millimeter-wave applications", IEEE Trans. Antennas Propag., vol. 69, no. 1, pp. 3-13, Jan. 2021.

[12] M. Bozzi, L. Perregrini, K. Wu, and P. Arcioni, “Current and future research trends in substrate integrated waveguide technology,” Radioengineering, vol. 18, pp. 201-209, June 2009.

[13] Zhi Ning Chen, Duixian Liu, Hisamatsu Nakano, Xianming Qing and Thomas Zwick, Handbook of Antenna Technologies: Wideband Magneto-electric Dipole Antennas, Singapore, 2015.

[14] K. B. Ng, H. Wong, K.K. So, C. H. Chan, and K. M. Luk, “60 GHz Plated Through Hole Printed Magneto-Electric Dipole Antenna,” IEEE Trans. Antennas Propag., vol. 60, no. 7, pp. 3129–3136, Jul. 2012.